Materials Chemistry and Physics 153 (2015) 365–375

Contents lists available at ScienceDirect

Materials Chemistry and Physics

journal homepage: www.elsevier.com/locate/matchemphys

Synthesis and characterization of hydrogels from 1-vinylimidazole. Highly resistant co-polymers with synergistic effect

Gastón A. Primo, María F. Garcia Manzano, Marcelo R. Romero, Cecilia I. Alvarez Igarzabal*

IMBIV-CONICET, Departamento de Química Orgánica, Facultad de Ciencias Químicas, Universidad Nacional de Córdoba, Haya de la Torre y Medina Allende, Edificio de Ciencias II, Ciudad Universitaria, Córdoba X5000HUA, Argentina

HIGHLIGHTS

- Highly resistant materials with improved mechanical properties can be obtained by adding 1-vinylimidazole as co-polymer.
- A synergistic effect can be observed by the combination of hydrophilic and hydrophobic monomers.
- The mechanical and swelling properties of different materials obtained were determined.

GRAPHICAL ABSTRACT

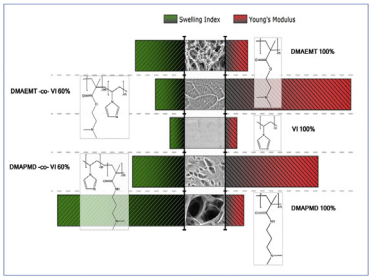

ARTICLE INFO

Article history:
Received 16 October 2014
Received in revised form
3 January 2015
Accepted 6 January 2015
Available online 8 January 2015

Keywords:
Polymers
Chemical synthesis
Mechanical testing
Mechanical properties

ABSTRACT

Monomers N, N-(dimethyl) amine ethyl methacrylate (DMAEMT) and N-[3 - (dimethylamine) propyl] methacrylamide (DMAPMD) were co-polymerized with 1-vinylimidazole (VI) in different proportions and crosslinked with N,N′-methylenebisacrylamide (BIS) in aqueous phase, to yield highly resistant hydrogels. The polymeric products were studied by swelling kinetics, solvent diffusion within the crosslinked network, thermal decomposition, *infrared spectroscopy* (*FTIR*), *variable pressure scanning electron microscopy* (*VP-SEM*), *and* mechanical and rheological tests. The incorporation of VI in the polymerization reaction led to beneficial changes in the properties of the final materials *such* as improvement in the resistance of the materials and increase in the percentage of deformation capable *of withstanding elongation before breaking. All VI-containing products were mechanically strong with* respect to homo-polymers (DMAPMD 100% and DMAEMT 100%). The most resistant products were DMAPMD-co-VI 60% and DMAEMT-co-VI 60%. A synergistic effect with the addition of VI is revealed by Young's modulus that *increases 5 and 10 times regarding the hydrogels yielded from pure monomers, respectively.*

1. Introduction

Functionalized polymers can be obtained by co-polymerization of monomers having different functional groups, or by post-modification of formed products in polymerization reactions [1–7]. Functionalized hydrophilic crosslinked materials capable of absorbing large amounts of water and containing functional groups (carboxylic acids, amines, hydroxyls, etc.) have been promising in their application as controlled-release systems for drugs, mechanical actuators, supports for tissue engineering, biomembrane systems, biosensors, chromatographic supports, metal ion complexing agents [8–12], among others. The application of these materials is sometimes restricted due to poor mechanical properties [13–15]. It mostly consists of water, which does not contribute to the

* Corresponding author.
E-mail address: cia@fcq.unc.edu.ar (C.I. Alvarez Igarzabal).

http://dx.doi.org/10.1016/j.matchemphys.2015.01.027
0254-0584/

mechanical strength of the gel. Due to their high water-holding capacity, polymer chains are widespread with low capacity for responding to an applied force, turning into particularly fragile materials [16–18]. However, the strength of the hydrogels can be improved by using different strategies. Some consist of increasing the density of crosslinks [19] or adding hydrophobic monomers to the polymer architecture [20], in order to generate higher-density areas or a larger amount of intermolecular interactions that contribute to increasing the module or stiffness of the hydrogels [21,22]. These modifications result in reducing the amount of water absorbed, for which compositions should be formulated by compromise between optimization of hydrophilicity and excellent mechanical properties [17]. For instance, gelatin films were stabilized by crosslinking with natural crosslinker genipin [23]; nano-sized attapulgite fibril was used to enhance the mechanical properties of polymeric hydrogels [24]; 2-vinyl-4,6-diamino-1,3,5-triazine was used in a co-polymerization to strengthen the mechanical properties of the hydrogel formed by self-hydrogen bonding of diaminotriazine [25]; ionically crosslinked alginate and covalently crosslinked polyacrylamide were mixed to yield extremely stretchable and tough hydrogels [26]; poly-(2-acrylamido-2-methyl-1-propane sulfonic acid) was combined with polyacrylamide [27] to yield double-network with excellent mechanical properties [28].

Other alternative to reinforce the structures of the hydrogel is the use of aromatic functional groups (in the constitutive monomers). In these systems, aromatic interactions play an important role [7] in maintaining the mechanical properties of the resulting hydrogels due to the rigidity of the backbone and the hydrophobicity of the aromatic segment [29]. Hence, obtaining a crosslinked structure with high strength, stiffness and toughness to resist failure would be advantageous over currently used materials [6,30–32].

1-vinylimidazole (VI) is a monomer with promising properties for modification of hydrogels [33]. Its aromatic structure and pH response have attracted the attention of researchers for numerous applications such as catalytic agent, metal-ion complexation, counter ion and dye binding [34,35]. Most of these applications have been tested with linear [36–41] and crosslinked polymers, using, however, VI as the constitutive monomer [42–46]. In addition, VI has not been almost used in those types of networks as a modifier capable of improving the texture or mechanical properties of the final materials [47]. The incorporation of VI into hydrogel structures has been regularly used especially in the formation of polymer-metal complexes used as immobilized catalysts [48–51].

The use of acrylate and acrylamide-based monomers is widespread in crosslinked materials [52]. In particular, 2-(dimethylamino) ethyl methacrylate (DMAEMT) and N-[3-(dimethylamino) propyl] methacrylamide (DMAPMD) are quite similar, except in their functionality (ester and amide, respectively). Hence, DMAEMT acts as a hydrogen-bond acceptor and DMAPMD acts as both hydrogen-bond acceptor and donor [53]. The aim of this paper thus focused on the analysis of the changes on properties based on the different possible interactions with VI, which could maximize structural freedom in highly steric environments [54].

Now, in general, of all possible applications, the use of hydrogels as complexing metal ions is highlighted since, once the polymer-metal complex ion is obtained, these can be used as supports for the immobilization of biomolecules, such as enzymes [55]. In turn, the study of ligands and polymers with supported metal complex derivatives is relevant in the field of catalytic and bio-organic chemistry [25].

Thus, the objective of the present study was the preparation of crosslinked hydrophilic co-polymers with specific functional groups in their structures using DMAPMD, DMAEMT and VI as monovinyl monomers and N,N'-methylenebisacrylamide (BIS) as a crosslinking agent. Different proportions of VI were incorporated into the polymer structures in order to yield mechanically strong hydrogels. A complete physico-chemical characterization of all the products was carried out with the purpose of using them in metal ion retention in future works.

2. Material and methods

2.1. Reagents

The following chemicals were used as purchased: N,N-dimethylaminoethyl methacrylate (DMAEMT; Sigma); *N*-[3-(dimethylamino)propyl]methacrylamide (DMAPMD; Aldrich); 1-vinylimidazole (VI; Aldrich); N,N'-methylenebisacrylamide (BIS; Sigma); ammonium persulphate (APS, Anedra); N,N,N′,N′-tetramethylethylenediamine (TEMED; Anedra); glacial acetic acid (CH_3COOH, Cicarelli); phosphoric acid (H_3PO_4, Cicarelli); boric acid (H_3BO_3, Cicarelli) and sodium hydroxide (NaOH, Cicarelli). Britton Robinson (BR) buffers were prepared according to reference [56]. The pH of each solution was adjusted at 3.02, 5.01, 7.00, 9.00 and 11.06.

2.2. Hydrogel synthesis

All matrices were prepared by free-radical cross-linking polymerization. The procedure for co-polymerization can be described as follows: monovinyl monomers (DMAEMT; DMAPMD and VI) and cross-linker (BIS) were dissolved in 4 mL of Milli-Q water in glass test tubes. The solution was mixed for 5 min and sonicated until complete homogenization. The polymerization solution was deoxygenated with N_2 for 5 min. To initiate the polymerization reaction, APS and 50% aqueous solution of TEMED were added to the reaction mixture and transferred to disposable syringes. The reaction was allowed to proceed for 1 day at room temperature. The synthesized hydrogels in rod form were cut into discs and thoroughly washed with Milli-Q water. They were then dried until constant weight. Table 1 summarizes the experimental conditions to prepare the hydrogels, and Fig. 1 shows monomer structures. The final products were named DMAPMD 100%; DMAPMD-co-VI 20%; DMAPMD-co-VI 60%; VI 100%; DMAEMT 100%; DMAEMT-co-VI 20% and DMAEMT-co-VI 60%, depending on molar co-monomer composition.

2.3. Swelling properties: dynamic, equilibrium and pH-response studies. Cycles of swelling and deswelling

The swelling indexes in equilibrium, q_w, were determined according to Eq. (1) where M_s and M_d are the mass of water-swollen hydrogel at equilibrium and the dry mass, respectively. To register

Table 1
Experimental conditions for the synthesis of hydrogels.

Hydrogel[a]	DMAPMD (mol 10^{-3})	DMAEMT (mol 10^{-3})	VI (mol 10^{-3})
DMAPMD 100%	5.60	–	–
DMAPMD-co-VI 20%	4.48	–	1.12
DMAPMD-co-VI 60%	2.24	–	3.36
VI 100%	–	–	5.60
DMAEMT 100%	–	5.60	–
DMAEMT-co-VI 20%	–	4.48	1.12
DMAEMT-co-VI 60%	–	2.24	3.36

[a] BIS: 1.1×10^{-3} mol; APS: 0.0128 g; 50% aqueous solution of TEMED: 0.5 mL; water: 4 mL.

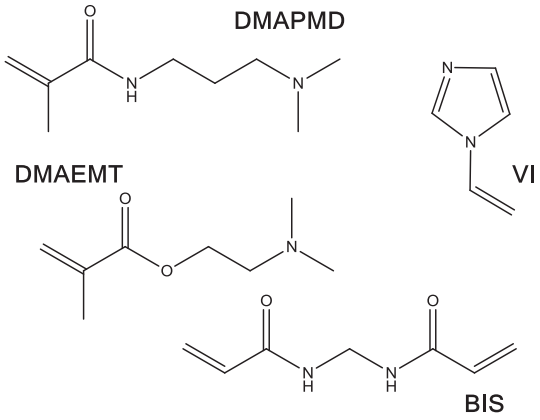

Fig. 1. Monomers used to prepare the hydrogels.

the kinetics of swelling in Eq. (1), M_s is replaced by M_t and measured every 10 min during the first 2 h and then every 30 min until constant weight.

$$q_w = M_s/M_d \quad (1)$$

The percentage of swelling ratio (% *SR*, Eq. (2)) in Milli-Q water versus time was plotted. M_t is the mass of water that diffused into the matrix at time *t*.

$$\%\, SR = [(M_t - M_d)/M_d]x100 \quad (2)$$

The water diffusion rate within the hydrogels was determined using Eq. (3), where M_∞ is the mass of water that diffuses into the matrix at the equilibrium, *k* is a constant associated with the network structure, and exponent *n* is a number related to the type of diffusion. This equation is applicable during the initial stages of swelling (<60%). The diffusion type (*n*) and *k* were calculated from the slope and intercept of the straight line, respectively, obtained from the plot of *ln F vs ln t*.

$$F = M_t/M_\infty = k\, t^n \quad (3)$$

From previous values, the diffusion coefficient (*D*) of water through the network can be obtained from Eq. (4) where *r* is the radius of the hydrogel in the dry state.

$$D = \pi r^2 (k/4)^{1/n} \quad (4)$$

The determination of the density of the hydrogels was performed by measuring the weight in n-heptane using the Archimedes principle.

To study the swelling in response to changes in the pH, the hydrogels were swollen at equilibrium in BR buffers [56] with a range of pH 2-11. The values of q_w were determined at each pH and plotted *vs* pH.

The swelling and deswelling cycles were determined by weightening dried hydrogel disks and placed to swell until swelling equilibrium in Milli-Q water. Subsequently, they were dried at 28 °C. This procedure was repeated systematically.

All the measurements were in triplicate and the values given by their averages.

2.4. Infrared spectroscopy (FTIR)

The samples in dry state were mixed with KBr and the infrared spectra (FTIR) were obtained on a Nicolet 5-SXC FTIR Spectrometer.

2.5. Rheological properties

The rheological characterization was performed using a rotational rheometer (Anton Paar-Physica MCR 301). The different tests were carried out using an 8 mm parallel plate. All assays were performed at 20 °C using a variable gap depending on the sample. The elastic (G') and the viscous (G'') moduli of the materials were measured using small amplitude oscillatory experiments.

The stress sweeps at a constant frequency of 10 Hz were performed on each sample to determine G' and G'' values and the linear viscoelastic region (LVR) profiles of each material by shearing them until the structure breakdown. Frequency sweeps at a constant stress were then applied to the samples over a wide range of frequencies (0.1–100 Hz) to study the viscoelastic performance of the hydrogels. No evidence of dehydration was found during the tests. All the measurements were in triplicate and the values given by their averages.

2.6. Compression test

The mechanical properties were analyzed with an Instron equipment (model 3342, Norwood, MA, USA). Cylindrical samples of gels (10 mm in diameter and variable height) were placed between flat metal surfaces fitted to Instron. The gels were compressed at 0.1 mm/s with compression force of increasing intensity up to the total breakdown of each sample. Then, real strain *vs* real stress was registered. The gel strength was characterized by failure strain, failure stress and initial Young's modulus. This last was calculated from the slope of the real strain *vs* real stress plot (stress not higher than 6%). All the measurements were performed in septuplicate and the values given by their averages.

2.7. Thermogravimetric analysis (TGA)

TGA was determined using dry samples (4–6 mg) at a scanning rate of 10 °C/min and analyzed in the range of 10–600 °C. The analyses were performed using a Hi-Res-TGA 2950, TA-Instruments, equipped with Universal analysis NT specific software.

2.8. Variable pressure scanning electron microscopy (VP-SEM) study

Samples were assembled in the sample holder and observed unmetallized. Micrographs were obtained with the aim of analyzing the morphology at a magnification of 400x. LEO 1450VP equipment was used.

3. Results and discussion

Novel hydrogels were synthesized by varying the ratio of comonomers used: DMAPMD 100%; DMAPMD-co-VI 20%; DMAPMD-co-VI 60%; VI 100%; DMAEMT 100%; DMAEMT-co-VI 20% and DMAEMT-co-VI 60%. Table 1 summarizes the experimental conditions. All polymers were obtained in rod form and were able to maintain the macroscopic structure after extraction from the reactors.

3.1. FTIR study

To characterize and analyze the hydrogels, FTIR spectra were performed (Fig. 2). The products formed by DMAPMD as base monomer have a strong signal at 1680 cm^{-1} corresponding to the vibration of C=O of amide group. Moreover, DMAEMT-based hydrogels have a strong signal at 1730 cm^{-1} corresponding to the vibration of C=O of the carbonyl of ester group. The signal at

1680 cm^{-1} can also be observed in the latter because the cross-linker BIS contains amide group and is part of all the products (Fig. 1). In all cases, except in 100% VI, the peaks at 2800 and 2900 cm^{-1} can be detected (vibration of N–CH_2 and N–CH_3, respectively).

For spectra of VI-containing products, the relative increase in the signals at 1430 and 610 cm^{-1} (stretching of C=N of the ring and C–N–C of VI, respectively) as percentage of VI increases can be observed. Furthermore, at greater proportions of DMAPMD or DMAEMT, the peaks at 2800 and 2900 cm^{-1} (N–CH_2 and N–CH_3 stetching, respectively) can be more clearly observed. In the spectra of products with increasing proportions of VI, especially in the case of DMAEMT-co-VI 60%, the signals at 1230 cm^{-1} (also present in VI 100%) are clearly observed, due to C–N bond stretching (of VI ring) and deformation (in plane) of CH (of VI ring). In addition, the signals at 1110 and 1084 cm^{-1} can be seen by the stretching of C–H bond of the ring.

3.2. Swelling properties and water diffusion parameters

In Table 2, both swelling properties and water diffusion parameters are shown. With respect to swelling indexes in equilibrium state, q_w, DMAPMD-containing hydrogels generally present higher swelling values in water. For the lower swelling value determined for VI 100%, it could be inferred that the chains are further compacted, as a result of the interaction between the imidazoline rings. While VI is being incorporated into the DMAPMD-co-VI structures, the swelling index decreases, due to structural changes that produce the aromatic rings, which probably causes decrease in pore size with respect to DMAPMD 100%.

Table 2
Swelling properties and water diffusion parameters for hydrogels.

Hydrogel	ρ (g mL^{-1})	q_w	n	D (10^{-8} m^2 s^{-1})
DMAPMD 100%	(1.11 ± 0.01)	(44 ± 1)	0.89	1.46
DMAPMD-co-VI 20%	(1.13 ± 0.01)	(30 ± 2)	0.79	1.97
DMAPMD-co-VI 60%	(1.15 ± 0.01)	(18 ± 1)	0.76	0.86
VI 100%	(1.18 ± 0.05)	(5 ± 2)	0.86	0.08
DMAEMT 100%	(1.10 ± 0.01)	(17 ± 2)	0.60	0.93
DMAEMT-co-VI 20%	(1.12 ± 0.01)	(14 ± 1)	0.58	0.75
DMAEMT-co-VI 60%	(1.16 ± 0.01)	(10 ± 1)	0.71	0.43

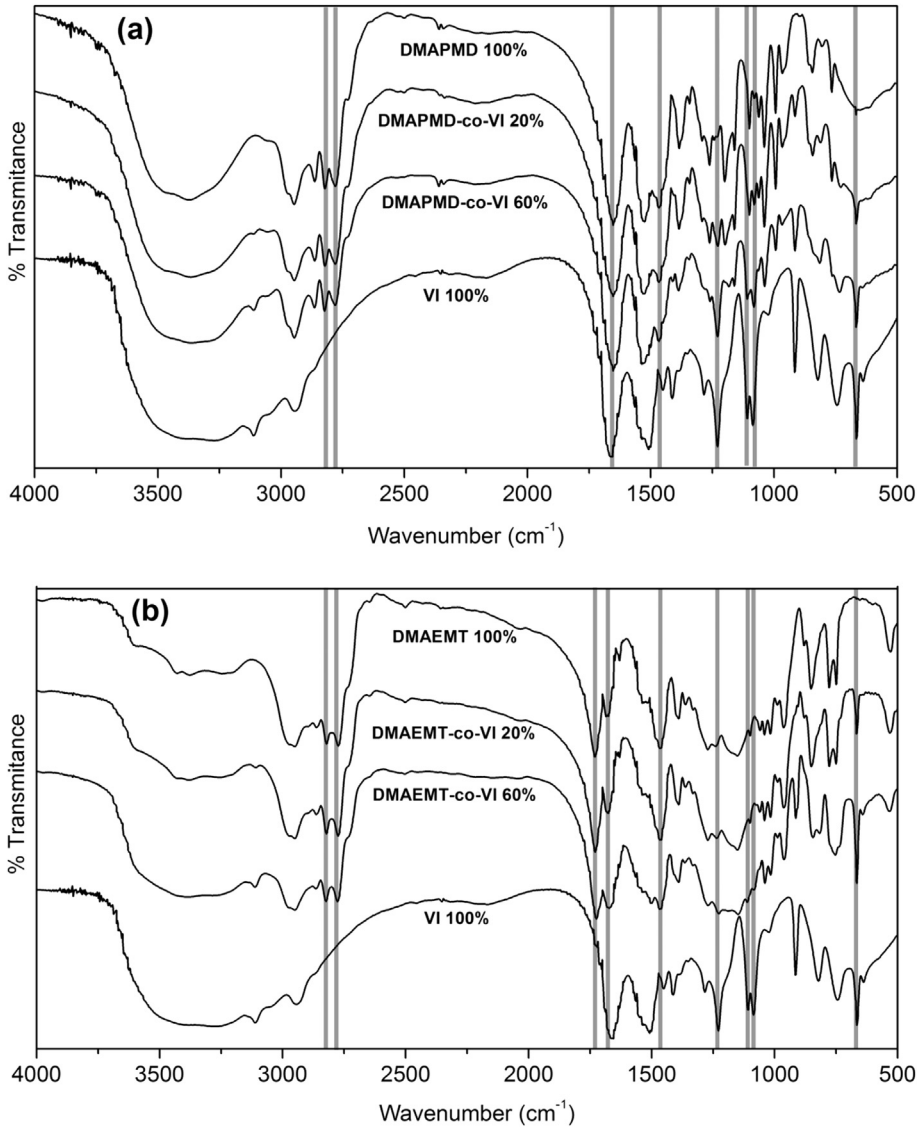

Fig. 2. FTIR spectra of (a) DMAPMD, (b) DMAEMT and co-polymers with VI.

DMAEMT-containing hydrogels were less swellable in water as compared with those containing DMAPMD. The incorporation of VI produced less marked decreases in swelling than that of previous ones.

The swelling kinetics in Milli-Q at 25 °C and neutral pH allows identifying the time for which the matrix and the solvent reach equilibrium swelling at those conditions. As shown in Fig. 3, DMAPMD-containing products and VI 100% hydrogels reached their maximum swelling rate at 1500 min (24 h approximately), while DMAEMT-containing products reached it in 2800 min (about 48 h).

Furthermore, knowing the diffusion coefficient (D) and the type of water (n) diffusion within the hydrogel involves important parameters for determining the interaction that occurs between the swelling solvent and the polymer chains. Table 2 lists the calculus of parameter n, which can take different values: $n = 0.45$ corresponds to Fickian-type diffusion (diffusion), $0.45 < n < 0.89$ corresponds to non-Fickian diffusion (diffusion and relaxation), $0.89 < n < 1$ responds to a diffusion type II (relaxation) and $n > 1$ corresponds to a super type II (plasticization). In the samples analyzed, n ranged between 0.58 and 0.89 indicating that the mechanism of penetration of water is controlled by diffusion and polymer chain relaxation (non-Fickian) [57]. Hydrogels in dry state have mostly hydrophobic chain–chain interactions. Upon contact with them, water molecules must break these interactions to favor the water–polymer interactions and generate more access or incorporation. Thus, each water molecule entering into the matrix produces a net pressure on the overall structure. Hydrogel chains must take time to respond to the swelling pressure and order themselves to reorder water molecules that enter and allow the entrance of more water within the structure.

The values of D (Table 2) have several orders of magnitude lower than those commonly found for free electrolyte in solution (10^{-6} m^2 s^{-1}) [58]. In these systems, water molecules have to diffuse into a polymer matrix, thus hindrance often occurs with the consequent decrease in D. VI 100% has the lowest diffusion coefficient and this could be produced by the strong interactions taking place between the imidazoline chain rings.

Table 2 shows the density measurements for the products. Density increases with the addition of VI possibly due to the favored hydrophobic interactions that generate a greater chain compaction, resulting in a higher ratio on the amount of material per volume unit.

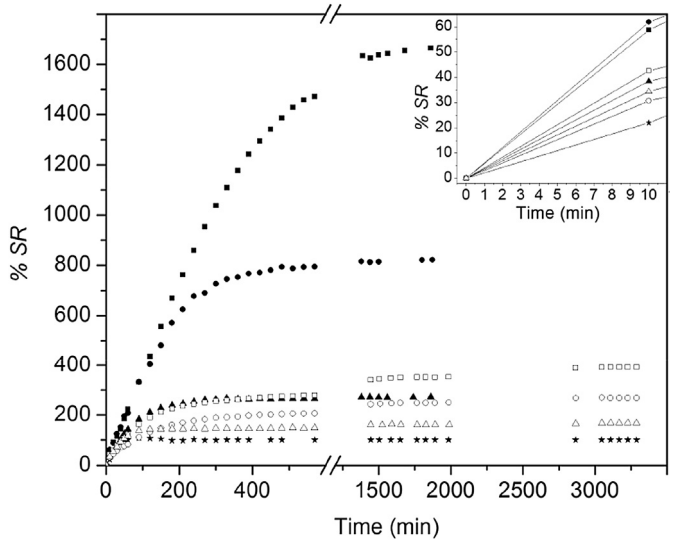

Fig. 3. Swelling kinetics determined in Milli-Q water for (■) DMAPMD 100%; (●) DMAPMD-co-VI 20%; (▲) DMAPMD-co-VI 60%; (□) DMAEMT 100%; (○) DMAEMT-co-VI 20%; (△) DMAEMT-co-VI 60% and (★) VI 100%.

3.3. Swelling pH-response

The macroscopic response of the hydrogels at different pHs is found in Fig. 4. As the pH increases, the products show a marked decrease in size. The major change in volume was observed for DMAEMT-co-VI 20%, in the range of pH 7-11. Regarding the functional groups in each matrix (Fig. 1), the imidazole and amide functional groups are protonated at pH < 7, generating electrostatic repulsions and causing further stretching of the polymer chains due to the net charge that must be supported; at very low pH values, they suffer major stretching. From Fig. 4, it can be noted that the repulsion generated by the functional groups at a low pH is high enough to yield a high degree of fragmentation (rupture). Except for DMAEMT-based products, at pH < 7 it was not possible to perform studies such as swelling index (q_w) due to loss of material in the process of surface drying.

Fig. 5 shows the swelling behavior of the products with the pH change. By increasing the pH, the hydrogels retain less water. Regular volume decrease was also observed with increasing pH in the homo-polymer DMAPMD 100% and when polymerized with VI, while a sharp drop in volume between pH 7 and 9 was observed for DMAEMT 100% and co-polymers DMAEMT-co-VI.

For DMAEMT-based hydrogels, pH variation generates different responses. The difference in q_w for the entire range of pH measured allows concluding that DMAEMT-based materials are less hydrophilic as compared with those based on DMAPMD.

The reversible response of products versus the applied force (LVR) can be particularly analyzed. Variation in pH did not produce significant changes in the LVR for DMAPMD 100%, DMAPMD-co-VI 20% and DMAPMD-co-VI 60% as shown in Fig. 6. Incorporating VI into the products generates a marked decrease in the LVR. In this case, VI would increase the elastic modulus G'; yet, the decrease in the LVR in concomitant form could indicate attractive short-range interactions between VI and DMAPMD (not electrostatic, since they are independent of pH). The LVR of DMAEMT 100% presents a rising response when pH increases. The incorporation of VI into DMAEMT-containing hydrogels decreases the LVR and the sensibility for pH variation. The combined effect of imidazole and acrylate in DMAEMT-co-VI 20% changes the materials conferring the capacity of resisting an applied force at great strain values.

LVR of DMAPMD-co-VI 60% depicts a minor extension as pH

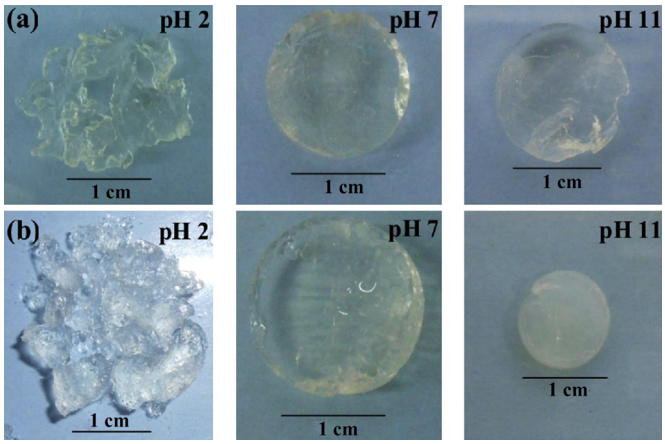

Fig. 4. Macroscopic response by (a) DMAPMD-co-VI 20% and (b) DMAEMT-co-VI 20% submitted to pH changes.

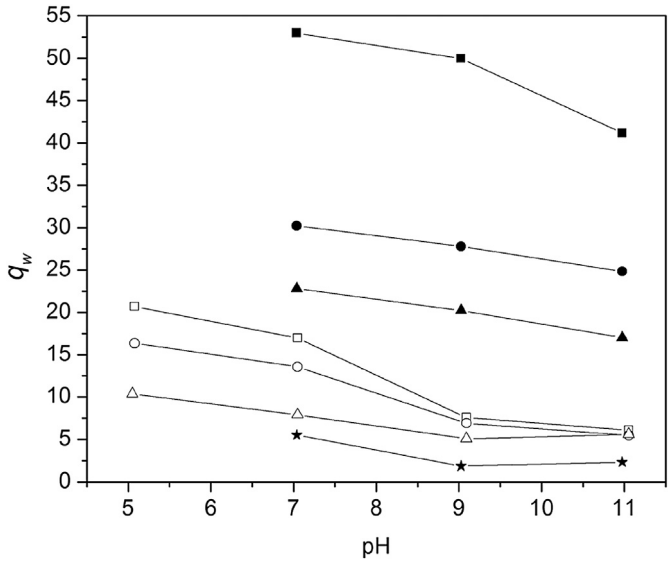

Fig. 5. Swelling response of hydrogels at different pH for (■) DMAPMD 100%; (●) DMAPMD-co-VI 20%; (▲) DMAPMD-co-VI 60%; (□) DMAEMT 100%; (○) DMAEMT-co-VI 20%; (△) DMAEMT-co-VI 60% and (★) VI 100%.

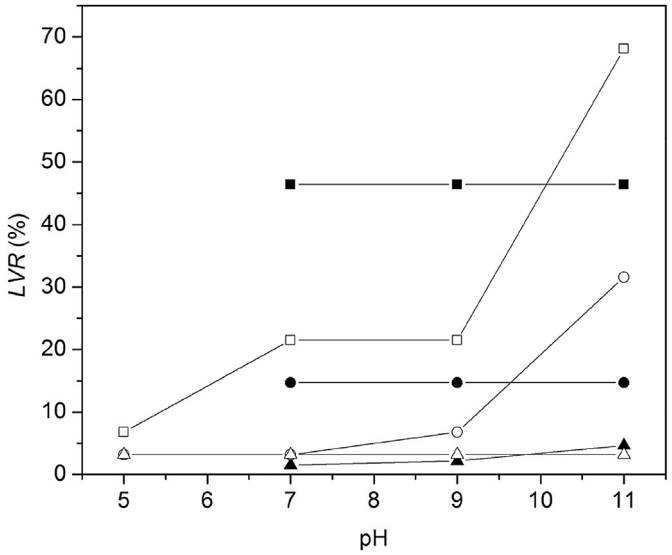

Fig. 6. LVR of products at different pH for (■) DMAPMD 100%; (●) DMAPMD-co-VI 20%; (▲) DMAPMD-co-VI 60%; (□) DMAEMT 100%; (○) DMAEMT-co-VI 20% and (△) DMAEMT-co-VI 60%.

increases since imidazoline aromatic rings produce a dominant effect as well as the ability to change shape against pH. DMAPMD-co-VI 60% and DMAEMT-co-VI 60% present particularly low values of reversible deformation. Irreversible deformation was detected up to 68.1 and 46.4%, respectively. The response observed could be attributed to the fact that aromatic rings produce a strong resonant planar interaction, decreasing chain flexibility. Thus, the three-dimensional network is highly compacted and constrained to displacement: when interactions break, the effect spreads throughout the structure causing its breakdown.

The high content of aromatic rings can produce a cooperative effect between them: once the resonant interaction between chains is interrupted by the force applied, they can again be rapidly rearranged by the high content of the functional groups and overcome the force applied reaching values in which the force is so great that the cooperative effect is lost and the material collapses completely.

3.4. Swelling and deswelling cycles

It is particularly important to know the possibility of reusability of the products compared to their ability to retain and expel water from the structure. Fig. 7 shows dry and swell weight of each material after several swelling/deswelling cycles.

At various cycles, DMAEMT-containing products proved more resistant than those formed by DMAPMD. This could be due to the low hydrophilic power of DMAEMT whose products presenting low swelling in water possess structures which not show significant changes from one state to another, thus the force that undergoes the polymeric chains in each process is less than that supported by the polymeric chains within DMAPMD-containing hydrogels. This produces low tolerarance to cycles, because of high levels of fracture (upper Fig. 7). Furthermore, the addition of VI develops lower resistance at the swelling / deswelling cycles generating ruptures in a fewer number of cycles. DMAEMT 100% and DMAEMT-co-VI 20% are capable of tolerating up to 16 swelling/deswelling cycles without significant changes in original mass and shape.

3.5. Rheological studies

Fig. 8 shows the amplitude sweep of DMAPMD-co-VI co-polymers. It could be seen that the addition of VI produces an increase in the storage module G' with respect to DMAPMD 100% and VI 100%. This indicates that, when both monomers are incorporated into the structures, the stiffness of the material increases, since G' values increase and more energy is required to deform it.

On comparison, two important aspects can be emphasized

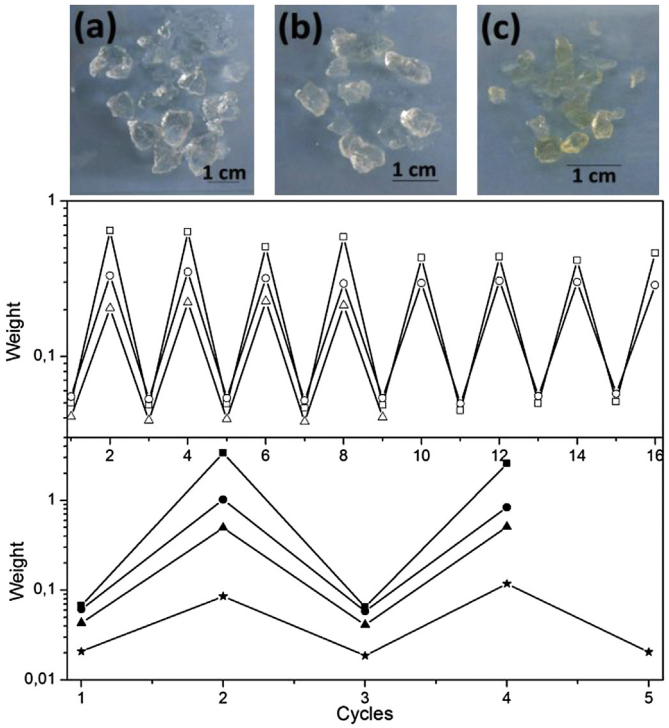

Fig. 7. Swelling/deswelling cycles in Milli-Q water for (■) DMAPMD 100%; (●) DMAPMD-co-VI 20%; (▲) DMAPMD-co-VI 60%; (□) DMAEMT 100%; (○) DMAEMT-co-VI 20%; (△) DMAEMT-co-VI 60% and (★) VI 100%. (Odd Cycle) Dry hydrogel; (Even Cycle) Swelling hydrogel. Up: Swelling hydrogels (a) DMAPMD 100%; (b) DMAPMD-co-VI 20% and (c) DMAPMD-co-VI 60%.

when DMAPMD 100% is modified with VI. First, the addition of VI increases LVR, which is expected considering that the aromatic rings of imidazoline type would provide more resistance to the deformation force as a consequence of the increased interaction between chains. Second, the viscous module G'' increases by the addition of VI as a co-monomer, remaining independent of the proportion. This response can be attributed to the low probability of chains to flow as a result of the interaction between imidazoline rings producing this effect even at low concentrations.

Fig. 9 shows the amplitude sweep of DMAEMT-co-VI co-polymers. In this case, the storage module also increases when VI is added as a co-monomer. The incorporation of VI in 60% of proportion leads to better mechanical properties. While the addition of co-monomer increases the strength capable of withstanding deformation, LVR decreases with respect to non-copolymerized materials. In turn, the general tendency is maintained in G'' mentioned in the case of DMAPMD-based products.

By performing a comparative analysis of both types of hydrogels, it was observed that DMAEMT 100% showed greater resistance to deformation and LVR as compared to DMAPMD 100%. Independently of the nature of the lateral chain, an increase in elasticity was observed for VI-containing co-polymers (particularly those containing 60% of VI) compared to DMAEMT 100% and DMAPMD 100%. It is worth mentioning that the elasticity of hydrogels with 60% of VI is higher than that of VI 100%. Hence, it could indicate the presence of favorable interactions between imidazole rings in the presence of amide or acrylate functional groups as hydrogen-bonds [54].

Figs. 10 and 11 show the response of each product according to the variation in the frequency of the oscillating force applied.

The complex viscosity (η^*) decays in proportion to the frequency, indicating that the elastic component of the material is greater than the viscous modulus. Thus, the materials exhibit marked solid component relative to the liquid, and are both independent of the frequency applied. Moreover, compared with the addition of VI, the same response can be seen in the analysis of amplitude sweeps, which confirms the increase in the resistance of the materials as co-polymers.

VI 100% deserves a particular analysis because, at very high frequencies, G' decays, rising then abruptly, while G'' is not detected. Although this behavior is atypical, it could be the result of the resistance provided by the imidazoline rings in the materials. At a high frequency, chains suffer a rearrangement process, causing an increase in the solid component as a result of the great stability of the inter-chain interactions generated by the rings. Initially, the drop could be attributed to the fact that the frequency oscillatory could generate motion between chains producing repulsion by the high electron density of imidazoline rings. Then, stability could be predominant on the repulsive effect, leading to an increase in the solid component (and hence in η^*) mentioned above. Finally, the materials do not show significant variation versus frequency in the force applied. Thus, the above discussion based on amplitude sweeps could apply to other frequency values between 0.1 and 100 Hz, not only to $\omega = 10$ Hz.

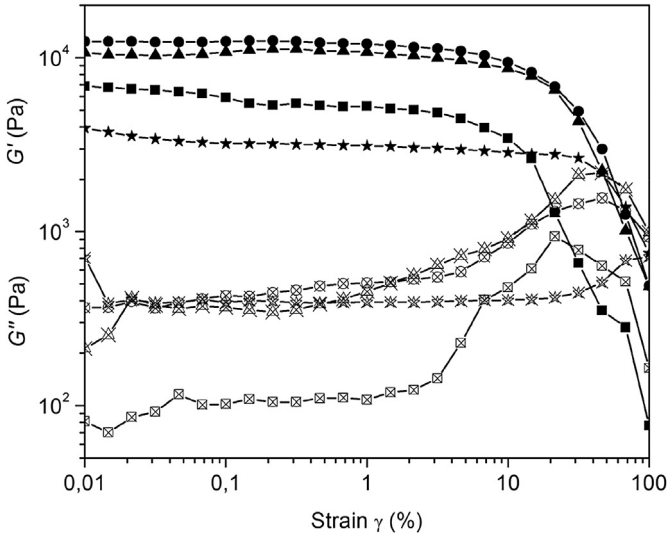

Fig. 8. Amplitude sweeps for (■ ⊠) DMAPMD 100%; (● ⊗) DMAPMD-co-VI 20%; (▲ ⧄) DMAPMD-co-VI 60%; and (★ ✳) VI 100%. (filled) G' (empty) G''.

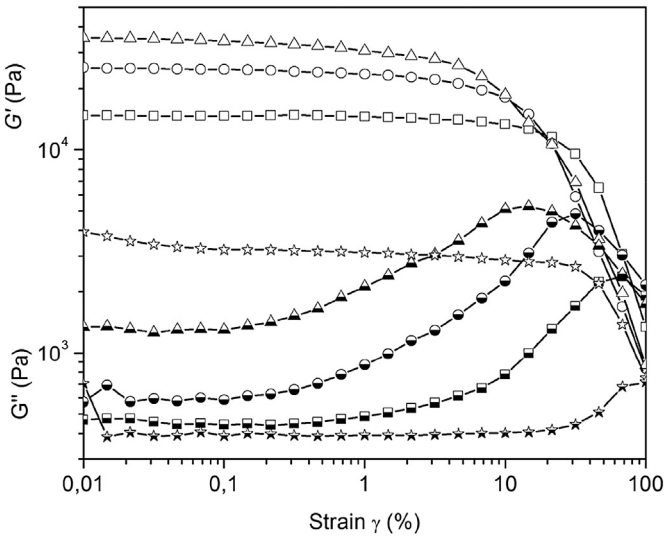

Fig. 9. Amplitude sweeps for (□ ⬓) DMAEMT 100%; (○ ◒) DMAEMT-co-VI 20%; (△ ⧋) DMAEMT-co-VI 60% and (☆ ✰) VI 100%. (empty) G' (half filled) G''.

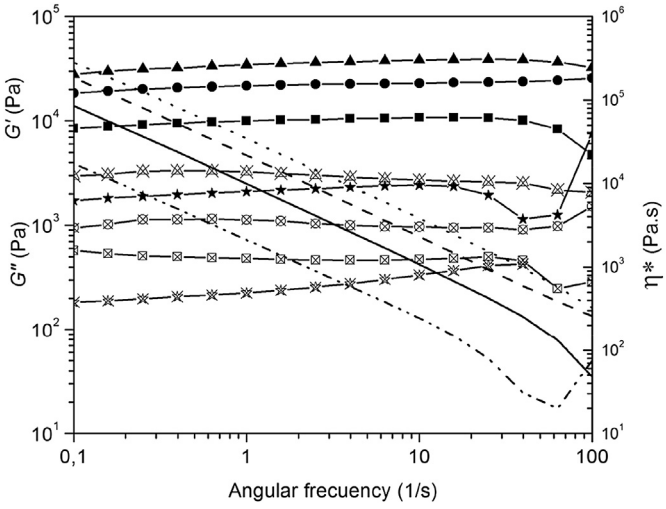

Fig. 10. Sweep frequency for (■ ⊠ ——) DMAPMD 100%; (● ⊗ —) DMAPMD-co-VI 20%; (▲ ⧄ ···) DMAPMD-co-VI 60%; and (★ ✳ ·-·-) VI 100%. (filled) G' (empty) G'' (lines) η^*.

3.6. Mechanical properties

Due to the viscoelastic nature of materials, mechanical characterization is important since it reveals relevant information. Table 3 shows the mechanical characteristics resulting from the different

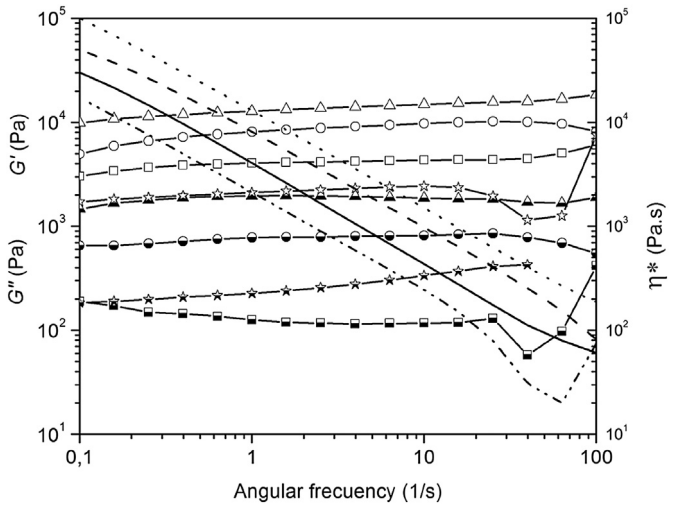

Fig. 11. Sweep frequency for (□ ■ ——) DMAEMT 100%; (○ ◒ —) DMAEMT-co-VI 20%; (△ ▲ ···) DMAEMT-co-VI 60% and (☆ ★ -·-·-) VI 100%. (empty) G' (half filled) G'' (lines) η^*.

hydrogels. It can be seen that the higher Young's moduli are reached by DMAEMT-based materials, and that as the proportion of VI into the structures is higher, this parameter increases. The moduli notably improve the mechanical properties produced by the addition of VI. The imidazoline ring could produce a greater interaction between the polymer chains of the materials by resonant effect, generating a reversible increase in resistance at a given compression force.

Moreover, from Fig. 12 it can be noted that the incorporation of VI improves the resistance of the materials and increases the percentage of deformation capable of withstanding elongation before total material breakdown. Table 3 details the strain to failure that can yield the products. The most resistant products were DMAPMD-co-VI 60% and DMAEMT-co-VI 60%. A synergistic effect with the adittion of VI is marked. Their Young's modulus increases 5 and 10 times with respect to the hydrogels yielded from pure monomers, respectively.

3.7. VP–SEM study

Considering the morphology of each material (Fig. 13), it can be stated that DMAPMD-containing hydrogels (Fig. 13 (a), (b) and (c)) have pores larger than those containing DMAEMT (Fig. 13 (d), (e) and (f)). In turn, the incorporation of VI into the products generate a large decrease in pore size until complete collapse of VI 100%, where no pore formation is observed.

DMAPMD-containing hydrogels have the higher q_w values (Table 2) in agreement with higher pore sizes observed in Fig. 13. With the addition of VI, q_w and pore size decrease. DMAEMT-containing hydrogels have smaller pores and q_w than those containing DMAPMD, reflecting their structural architecture. Thus, pore size can be related to the space available to the entrance of water into the material. Pore size observed by VP-SEM is in agreement with the diffusion coefficients shown in Table 2. VI 100% has the higher density (Table 2) and this property decreases with the incorporation of the co-monomer. This agrees with Fig. 13 (g): in a given volume, the amount of matter in VI 100% is compacted and higher than in those materials with porous structure. To summarize, Table 2 and Fig. 13 show the consequence of incorporating VI in the porosity of products. VI creates attractive interactions in the hydrogels containing DMAPMD and DMAEMT and, as a consequence, pore size decreases with the incorporation of this co-monomer.

Thus, data shown in Table 2 are consistent with those from studies of the morphology of each material. The specific structure determines the final properties of each material independently of chemical composition.

Table 3
Mechanical properties determined for the materials.

Hydrogel	Young modulus (kPa)	Failure strain (kJ/m^3)
DMAPMD 100%	522.5	69.5
DMAPMD-co-VI 20%	609.0	529.6
DMAPMD-co-VI 60%	2602.5	12,610.9
DMAEMT 100%	635.8	5349.0
DMAEMT-co-VI 20%	664.4	8542.7
DMAEMT-co-VI 60%	3515.6	11,977.8
VI 100%	334.4	377.7

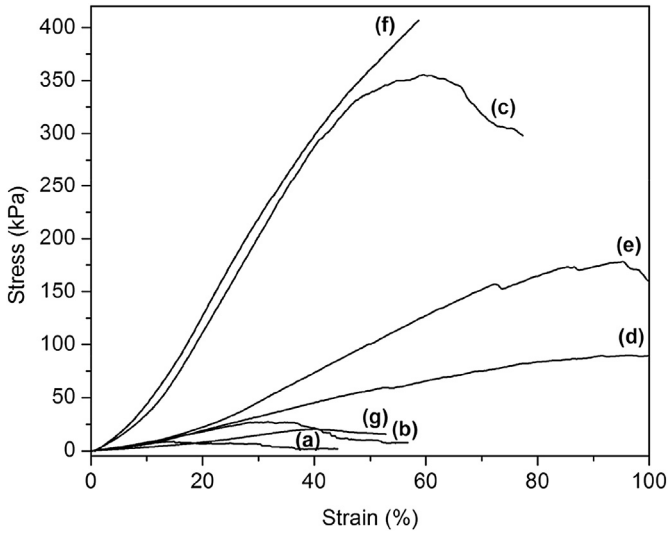

Fig. 12. Mechanical response for (a) DMAPMD 100%; (b) DMAPMD-co-VI 20%; (c) DMAPMD-co-VI 60%; (d) DMAEMT 100%; (e) DMAEMT-co-VI 20%; (f) DMAEMT-co-VI 60% and (g) VI 100%.

3.8. TGA study

Although the three-dimensional structure of the hydrogels and their properties correspond to the swollen state, knowing their thermal stability is important for certain applications where products may be exposed to high temperature. Starting from dry products, Table 4 shows that all present 13.5–2.2% of water strongly retained (depending on the specific composition) is not likely to be removed by drying at 28 °C possibly due to solvatation of polymer chains or by diffusional impediments. Furthermore, the higher hydrophilicity of DMAPMD with respect to that of DMAEMT can be clearly noted since DMAPMD-containing products present higher values of q_w (Table 2) and lower elastic modulus values (Section 3.5). Additionally, DMAPMD-containing hydrogels exhibit higher loss of water at 100 °C compared to those formed from DMAEMT.

As shown in Table 4, VI 100% retained the larger percentage of water. Nevertheless, swelling indexes did not show the same response (Table 2), indicating the strong attractive interactions between the polymer chains in the hydrogel structure. The incorporation of VI into network structures to form co-polymers also increases the capacity of water retention. The q_w does not reflect hidrofilicity increase, thus attractive interactions are greater than

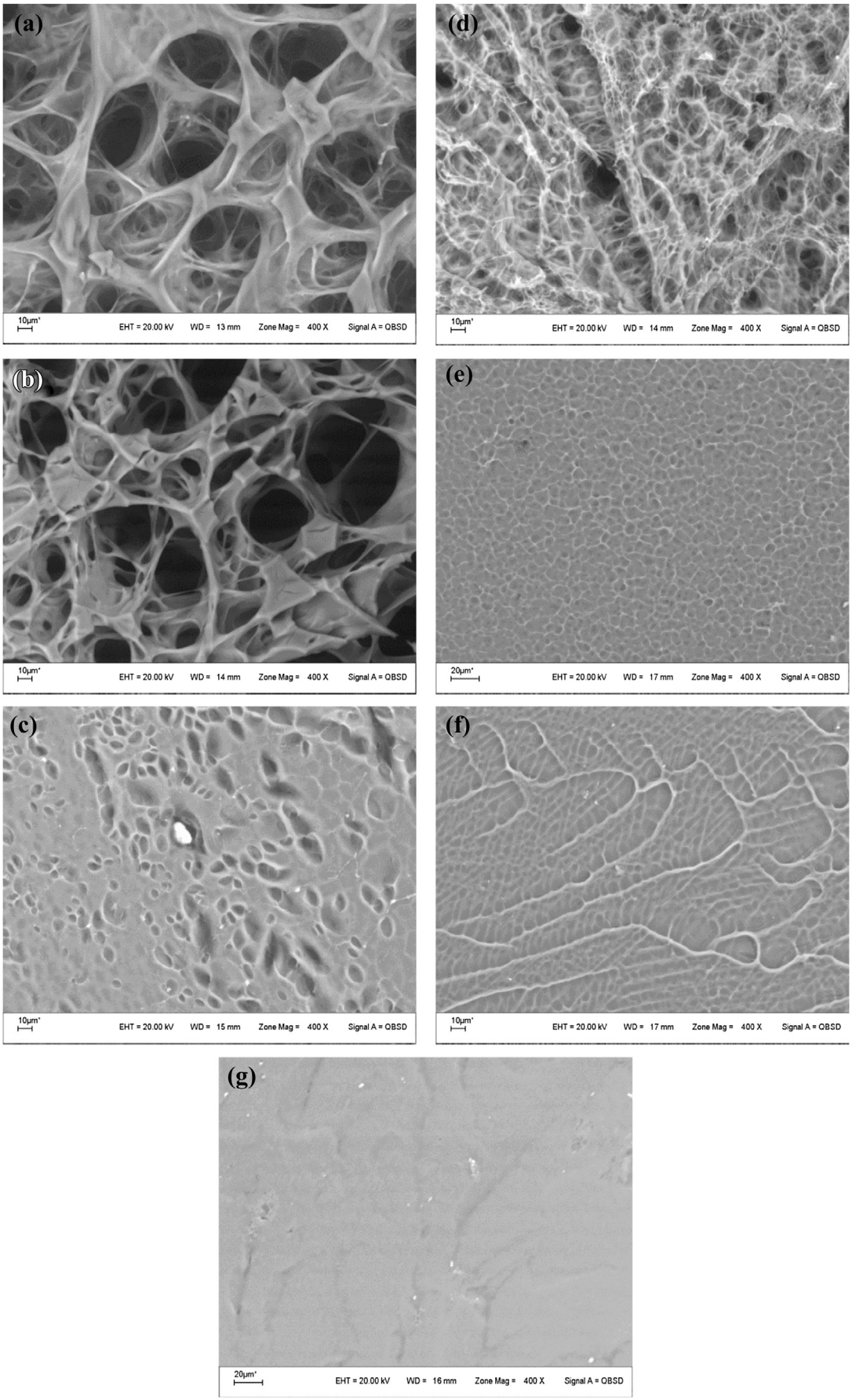

Fig. 13. VP-SEM micrographs (400x) of (a) DMAPMD 100%, (b) DMAPMD-co-VI 20%, (c) DMAPMD-co-VI 60%, (d) DMAEMT 100%, (e) DMAEMT-co-VI 20%, (f) DMAEMT-co-VI 60% and (g) VI 100%.

Table 4
[a]Decomposition study (temperature and percentages) of the products.

Hydrogel	Water strongly retained (%)	Decomposition temperature (°C)		Decomposition (%)
DMAPMD 100%	7.92	277.01		83.10
DMAPMD-co-VI 20%	9.60	267.15		85.23
MAPMD-co-VI 60%	9.60	241.05		80.41
VI 100%	13.54	293.52		58.41
DMAEMT 100%	2.19	201.16	370.68	87.15
DMAEMT-co-VI 20%	2.86	197.12	351.07	84.52
DMAEMT-co-VI 60%	7.11	174.29	336.81	81.48

[a] TGA spectra on supplementary information.

those with water molecules.

After materials suffer loss of water strongly retained at temperatures near 100 °C, the structures remain stable over a wide range of temperatures. Their decomposition temperatures are summarized in Table 4. The decomposition of DMAPMD 100% and DMAEMT 100% occurs in one and two steps, respectively.

All hydrogels except VI 100% suffer approximately 85% of matter loss with respect to their original weight. Thus, it is concluded that DMAEMT- or DMAPMD-containing hydrogels form a large amount of volatiles with respect to VI 100%, indicating increased stability of this last product to at least 500 °C.

4. Conclusions

The preparation of crosslinked hydrophilic co-polymers with specific functional groups in their structure using DMAPMD and DMAEMT as monovinyl monomers and BIS as a crosslinking agent was performed. Different proportions of VI were incorporated into the polymer structures in order to yield mechanically strong hydrogels. The strength of failure, Young's modulus and elastic modulus (G') increase when VI fraction is 0.6, whether or not the other co-monomer is DMAEMT or DMAPMD. The q_w values decrease with the increase in the mole fraction of VI independently of the co-monomer, indicating that interactions between chains are intensified by the presence of VI. The addition of VI increases the amount of water retained for both amide and acrylate based-co-polymers. This not only indicates that VI favors attractive interactions, it is also favored with the solvent.

Probably, the synergistic effect is not caused by amides or ester groups present in DMAPMD and DMAEMT, respectively (since increase is similar in both cases). It is likely that favorable interactions occur between VI and DMAPMD and DMAEMT monomers because the determinations of failure strength resulted higher than their respective homo-polymers. The observed proportion of greater synergy, which is 3: 2 (VI:co-monomer), would indicate another probable cause. Therefore, DMAEMT or DMAPMD could act as spacers of the imidazole rings, increasing Young's module and failure strength. However, the swelling-deswelling effect can produce great changes between the distance of the chains. This could explain the presence of the lower viscoelastic range based on the short range of VI ring interactions.

These optimized materials, with highly proved synergistic effect, are being tested in application such as metal ion complexation agent, enzyme immobilization and hydrogen peroxide decomposition. The results will be shown in a future work.

Acknowledgments

Authors acknowledge Consejo Nacional de Investigaciones Cientificas y Tecnicas (CONICET), SECyT (Universidad Nacional de Córdoba) and FONCyT for financial assistance. G. A. Primo and M. F. Garcia Manzano also acknowledge receipt of fellowships from CIN and CONICET, respectively.

Appendix A. Supplementary data

Supplementary data related to this article can be found at http://dx.doi.org/10.1016/j.matchemphys.2015.01.027.

References

[1] M.M. Sadat Ebrahimi, H. Schönherr, Langmuir 30 (2014) 7842–7850.
[2] S. Emik, React. Funct. Polym. 75 (2014) 63–74.
[3] D.K. Wang, S. Varanasi, P.M. Fredericks, D.J.T. Hill, A.L. Symons, A.K. Whittaker, F. Rasoul, J. Polym. Sci. Part A: Polym. Chem. 51 (2013) 5163–5176.
[4] P.N. Moghadam, R. Hasanzadeh, J. Khalafy, Iran. Polym. J. 22 (2013) 133–142.
[5] S.J. Buwalda, P.J. Dijkstra, J. Feijen, J. Polym. Sci. Part A: Polym. Chem. 50 (2012) 1783–1791.
[6] G. Bayramoglu, V. Bitirim, Y. Tunali, M.Y. Arica, K.C. Akcali, Mater. Sci. Eng. C. 33 (2013) 801–810.
[7] V. Jayawarna, S.M. Richardson, A.R. Hirst, N.W. Hodson, A. Saiani, J.E. Gough, R.V. Ulijn, Acta Biomater. 5 (2009) 934–943.
[8] B. Osman, A. Kara, L. Uzun, N. Besirli, A. Denizli, J. Mol. Catal. B: Enzym 37 (2005) 88–94.
[9] E. Ramírez, S.G. Burillo, C. Barrera-Diaz, G. Roa, B. Bilyeu, J. Hazard. Mater. 192 (2011) 432–439.
[10] B.M.A. Carvalhoa, S.L. Da Silva, L.H.M. Da Silva, V.P.R. Minim, M.C.H. Da Silva, L.M. Carvalho, L.A. Minim, Sep. Purif. Rev. 43 (2014) 241–262.
[11] A. Kowalczyk, M. Fau, M. Karbarz, M. Donten, Z. Stojek, A.M. Nowicka, Biosens. Bioelectron. 54 (2014) 222–228.
[12] J.L. Morán-Quiroz, E. Orozco-Guareño, R. Manríquez, G.G. Carbajal-Arízaga, W. de la Cruz, S. Gomez-Salazar, J. Appl. Polym. Sci. 131 (2014), http://dx.doi.org/10.1002/app.39933.
[13] R. Mao, J. Tang, B.G. Swanson, Carbohyd. Poly 41 (2000) 331–338.
[14] A.M. Kloxin, C.J. Kloxin, C.N. Bowman, K.S. Anseth, Adv. Mater. 22 (2010) 3484–3494.
[15] T. Sakai, T. Matsunaga, Y. Yamamoto, C. Ito, R. Yoshida, S. Suzuki, N. Sasaki, M. Shibayama, U. Chung, Macromolecules 41 (2008) 5379–5384.
[16] D.M. Li, Z. Zhang, K.M. Liew, Comput. Methods Appl. Mech. Engrg 274 (2014) 84–102.
[17] L.E. Nielsen, R.F. Landel (Eds.), Mechanical Properties of Polymers and Composites, second ed., M. Dekker, New York, 1994.
[18] M. Shibayama, Macromol. Chem. Phys. 199 (1998) 1–30.
[19] M.C. Straccia, I. Romano, A. Oliva, G. Santagata, P. Laurienzo, Carbohyd. Poly 108 (2014) 321–330.
[20] D.G. Papageorgiou, D.N. Bikiaris, K. Chrissafis, Thermochim. Acta 543 (2012) 288–294.
[21] S. Cram, H. Brown, G. Spinks, D. Hourdet, C. Creton, in: Proceedings of the SPIE International Symposium, 2004. Sydney.
[22] Y. Li, M. Qin, Y. Cao, W. Wang, Sci. China: Phys. Mech. Astron 57 (2014) 849–858.
[23] A. Bigi, G. Cojazzi, S. Panzavolta, N. Roveri, K. Rubin, Biomaterials 23 (2002) 4827–4832.
[24] Y. Wang, D. Chen, J. Colloid Interface Sci. 372 (2012) 245–251.
[25] N. Wang, Y. Han, Y. Liu, T. Bai, H. Gao, P. Zhang, W. Wang, W. Liu, J. Hazard. Mater. 213-214 (2012) 258–264.
[26] Je Sun, X. Zhao, W.R.K. Illeperuma, O. Chaudhuri, K.H. Oh, D.J. Mooney, J.J. Vlassak, Z. Suo, Nature 489 (2012) 133–136.
[27] J.P. Gong, Soft Matter 6 (2010) 2583–2590.
[28] T. Tominaga, V.R. Tirumala, E.K. Lin, J.P. Gong, H. Furukawa, Y. Osada, W. Wu, Polymer 48 (2007) 7449–7454.
[29] G. Tronci, A. Doyle, S.J. Russell, D.J. Wood, J. Mater. Chem. B 1 (2013) 5478–5488.
[30] A.L. DiRienzo, C.M. Yakacki, M. Frensemeier, A.S. Schneider, D.L. Safranski, A.J. Hoyt, C.P. Frick, J. Mech. Behav. Biomed. Mater. 30 (2014) 347–357.
[31] I. Kavianinia, P.G. Plieger, N.G. Kandile, D.R.K. Harding, Carbohyd. Poly 87 (2012) 881–893.
[32] J. He, S. Machida, H. Kishi, K. Horie, H. Furukawa, R. Yokota, J. Polym. Sci. Part A: Polym. Chem. 40 (2002) 2501–2512.
[33] B.L. Rivas, H.A. Maturana, M.J. Molina, M.R. Gómez-Antón, I.F. Piérola, J. Appl. Polym. Sci. 67 (1998) 1109–1118.
[34] G. Chen, K.K.S. Lau, K.K. Gleason, Thin Solid Films 517 (2009) 3539–3542.
[35] M.H. Wahdan, G.K. Gomma, Mater. Chem. Phys. 47 (1997) 176–183.
[36] W. Zhang, H. Wang, B. Shentu, C. Gu, Z. Weng, J. Appl. Polym. Sci. 120 (2011) 109–115.
[37] N. Pekel, H. Savas, O. Güven, Colloid Polym. Sci. 280 (2002) 46–51.
[38] H. Caner, E. Yilmaz, O. Yilmaz, Carbohyd. Poly 69 (2007) 318–325.
[39] H. El-Hamsharya, M.M.G. Foudaa, M. Moydeena, S.S. Al-Deyab, Int. J. Biol. Macromol. 66 (2014) 289–294.
[40] H. Ibrahim Unal, O. Erol, O. Yunus Gumus, Colloids Surf. A 442 (2014) 132–138.
[41] J. Shin, S.G. Han, W. Lee, Anal. Chim. Acta 752 (2012) 87–93.
[42] A. Domján, C. Fodor, S. Kovács, T. Marek, B. Iván, K. Süvegh, Macromolecules

45 (2012) 7557–7565.
[43] M.J. Molina, M.R. Gómez-Antón, I.F. Piérola, J. Polym. Sci. Part B: Polym. Phys. 42 (2004) 2294–2307.
[44] Ö.B. Üzüm, E. Karadag, J. Polym. Res. 14 (2007) 483–488.
[45] B. Isik, B. Dogantekin, J. Appl. Polym. Sci. 96 (2005) 1783–1788.
[46] E.B. Anderson, T.E. Long, Polymer 51 (2010) 2447–2454.
[47] L. Carr, G. Cheng, H. Xue, S. Jiang, Langmuir 26 (2010) 14793–14798.
[48] N. Pekel, B. Salih, O. Güven, J. Biomater. Sci. Polym. Ed. 16 (2005) 253–266.
[49] N. Pekel, B. Salih, O. Güven, J. Mol. Catal. B: Enzym 21 (2003) 273–282.
[50] S. Akgöl, N. Öztürk, A.A. Karagözler, D.A. Uygun, M. Uygun, A. Denizli, J. Mol. Catal. B: Enzym 51 (2008) 36–41.
[51] K.H. Park, D.H. Lee, K. Na, Biotechnol. Lett. 31 (2009) 337–346.
[52] G. Amidon, P.I. Lee, E.M. Topp (Eds.), Transport Process in Pharmaceutical Systems, Marcel Dekker Inc, 2000.
[53] J. De Ruiter, in: Principles of Drug Action, Springer, 2005.
[54] A. Cammers, S. Parkin, Cryst. Eng. Comm. 6 (2004) 168–172.
[55] N. Sahiner, S. Butun, O. Ozay, B. Dibek, J. Colloid Interface Sci. 373 (2012) 122–128.
[56] T. Çaykara, R. İnam, J. Appl. Polym. Sci. 91 (2004) 2168–2175.
[57] N.A. Peppas, P. Bures, W. Leobandung, H. Ichikawa, Eur. J. Pharm. Biopharm. 50 (2000) 27–46.
[58] M.H. Friedman, in: Principles and Models of Biological Transport, second ed., Springer, 2008.